

# Geophysical Research Letters<sup>®</sup>

## RESEARCH LETTER

10.1029/2022GL100369

### Key Points:

- Day-to-day variability of the semidiurnal tide in the F-region plasma resolved
- Strength of polar vortex impacts ionosphere in both hemispheres on a day-by-day basis
- Stratospheric winds variation of <10 m/s change ionospheric plasma tides by a factor of 2

### Correspondence to:

J. Oberheide,  
[joberhe@clemson.edu](mailto:joberhe@clemson.edu)

### Citation:

Oberheide, J. (2022). Day-to-day variability of the semidiurnal tide in the F-region ionosphere during the January 2021 SSW from COSMIC-2 and ICON. *Geophysical Research Letters*, 49, e2022GL100369. <https://doi.org/10.1029/2022GL100369>

Received 14 JUL 2022  
Accepted 29 AUG 2022

## Day-to-Day Variability of the Semidiurnal Tide in the F-Region Ionosphere During the January 2021 SSW From COSMIC-2 and ICON

J. Oberheide<sup>1</sup> 

<sup>1</sup>Department of Physics and Astronomy, Clemson University, Clemson, SC, USA

**Abstract** The semidiurnal tidal spectrum in the F-region ionosphere obtained from hourly COSMIC-2 Global Ionospheric Specification (GIS) data assimilation is greatly (>50%) enhanced during the January 2021 Sudden Stratospheric Warming (SSW). Moreover, the semidiurnal migrating tidal response in topside electron densities closely follows the day-to-day changes of the 10 hPa, 60°N zonal wind from MERRA-2 during the SSW. The response is similar in the northern and southern crests of the Equatorial Ionization Anomaly (EIA) but persists toward higher magnetic latitudes and the EIA trough. A slight phase shift toward earlier local times is consistent with theoretical expectations of an E-region dynamo driving and agrees with semidiurnal tidal diagnostics of MIGHTI/ICON zonal winds at 105 km. COSMIC-2 GIS are the first data set to resolve the tidal weather of the ionosphere on a day-to-day basis and, therefore, provide a new perspective on space weather variability driven by lower and middle atmosphere dynamics.

**Plain Language Summary** Understanding the coupling between the weather of the troposphere and stratosphere with the space weather of the ionosphere has been one of the yet unsolved science challenges over the past decade. While progress has been made on seasonal and subseasonal timescales, the lack of sufficient global local time coverage data prevented further progress. The Constellation Observing System for Meteorology, Ionosphere, and Climate 2 (COSMIC-2) constellation now enables the community to make the next step and resolve global-scale ionospheric variability every hour. An unexpected finding is that even small wind changes (<10 m/s) in the stratospheric polar vortex region are closely mapped into the global F-region, changing semidiurnal electron density amplitudes by almost a factor of two (peak-to-peak) within a few days.

## 1. Introduction

Much work has been done in the past decade to study the response of the low latitude ionosphere to Sudden Stratospheric Warmings (SSWs), that is, a temporary break-up of the polar vortex in the stratosphere, which itself is a result of polar jet stream wobbles caused by Rossby waves. SSW related strato-/mesospheric wind and temperature changes cause a resonant amplification of the lunar semidiurnal migrating tide (M2, 12.42 hr) because of the atmospheric Pekeris mode (Forbes & Zhang, 2012), and a solar semidiurnal migrating tide (SW2, 12 hr) enhancement due to stationary planetary wave interactions (e.g., Sathishkumar & Sridharan, 2013, and others) and changes in the tidal propagation and ozone forcing of SW2 (e.g., Jin et al., 2012, and others). The pioneering work by Goncharenko et al. (2010) showed that these semidiurnal enhancements substantially modify the low latitude F-region ionosphere, mainly through tidally driven E-region dynamo changes with resulting mapping of polarization electric fields into the F-region and vertical plasma drifts. SSWs also change the mean state of the thermosphere, that is, in thermospheric composition. Thermosphere Ionosphere Electrodynamic General Circulation Model (TIE-GCM) simulations by Yamazaki and Richmond (2013) hypothesized that enhanced tides cause more wave breaking in the lower thermosphere, thus setting up an upward/poleward two-cell circulation in the lower thermosphere that depletes atomic oxygen. Molecular diffusion then propagates the depleted atomic oxygen throughout the whole thermosphere, causing a roughly 20% reduction of daytime mean O/N<sub>2</sub> column densities. This was recently confirmed by Global-scale Observations of the Limb and Disk (GOLD) observations made during the 2019 SSW (Oberheide et al., 2020).

An outstanding science challenge in researching the SSW impact on the upper atmosphere is the lack of suitable global observations that allow one to resolve the tidal winds in the E-region dynamo on a daily basis, that is, the “tidal weather.” Single satellite tidal wind diagnostics such as from the TIMED Doppler Interferometer on the Thermosphere Ionosphere Mesosphere Energetics and Dynamics satellite (TIDI/TIMED) (Oberheide

© 2022. The Authors.

This is an open access article under the terms of the [Creative Commons Attribution-NonCommercial License](https://creativecommons.org/licenses/by-nc/4.0/), which permits use, distribution and reproduction in any medium, provided the original work is properly cited and is not used for commercial purposes.

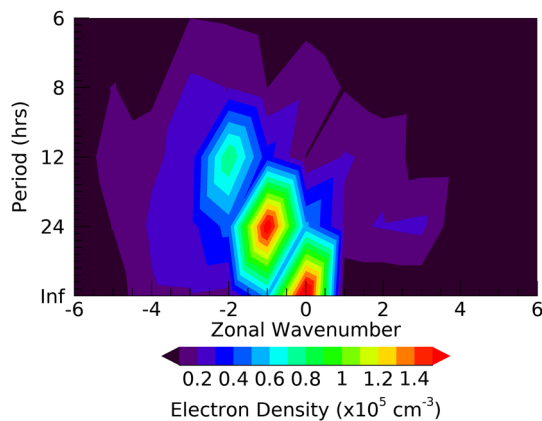


**Figure 1.** Tidal amplitude spectrum on 6 January 2021, at 380 km and 20°N magnetic latitude, from the COSMIC-2 GIS data set. Negative wavenumbers correspond to westward propagating waves and positive wavenumbers to eastward propagating waves.

et al., 2011) or more recently from the Michelson Interferometer for Global High-resolution Thermospheric Imaging on the Ionospheric Connection Explorer (MIGHTI/ICON) (Forbes et al., 2022) can only resolve tidal variations on a monthly or longer timescale, similar to lunar tidal diagnostics from ICON and GOLD (Lieberman et al., 2022). Consequently, SSW variations, while still present, are considerably smoothed in MIGHTI/ICON tidal diagnostics. Data assimilation in the mesosphere/lower thermosphere, that is, from systems like the Navy Global Environmental Model–High Altitude (NAVEM–HA), can partly mitigate this challenge and provide realistic day-to-day tidal variations close to the E-region during SSW (Lieberman et al., 2015; Liu et al., 2022). Space-based global-scale wave diagnostics in the ionosphere in response to a SSW has been limited to planetary wave periods (e.g., Yamazaki et al., 2020, and others) due to the inherent limitations of single satellites or small constellations with insufficient local time resolution to diagnose the ionospheric tides on sub-monthly time scales. Previous work using Global Positioning System based total electron content maps and earlier COSMIC-1 based GIS data was also largely focused on planetary wave period variability in SW2 and various nonmigrating tidal components (e.g., N. M. Pedatella & Forbes, 2010; J. T. Lin et al., 2019, and others).

This manuscript utilizes the new Constellation Observing System for Meteorology, Ionosphere, and Climate 2 (COSMIC-2) data to close this gap in our understanding of the ionospheric tidal response by utilizing hourly electron density profiles from the Global Ionospheric Specification (GIS) data product. The target is the January 2021 SSW, characterized by 10 hPa, 60°N zonal winds that reversed between 5-January and 2-February with peak on 15-January and some intermittency. The semidiurnal tidal spectrum shows substantial day-to-day variations that are conclusively mapped to polar stratospheric wind variations with the help of MIGHTI/ICON E-region tidal winds. The observed ionospheric tidal variations are unrelated to geomagnetic and solar variations. The results clearly show that even comparatively small wind variations in the polar vortex region have a large impact on the low latitude ionosphere, perhaps even more so than previously thought by the community and reported in the literature.

## 2. COSMIC-2 GIS Data and Tidal Diagnostics

The COSMIC-2 six satellite mission was launched on 25 June 2019 into a ~24° inclination orbit. It provides in-situ electron density from the Ion Velocity Meter (IVM) instrument and thousands of daily Radio Occultation (RO) soundings. The satellites reached their final configuration near 530 km with a ~60° longitude separation (C. Y. Lin, Lin, et al., 2020) in February 2021. GIS electron density is the hourly data product based on the Gauss-Markov Kalman filter (C. Y. Lin et al., 2017), assimilating the ground-based Global Positioning System and space-based COSMIC-2 RO slant total electron content. GIS data are on 5° × 2.5° × 20 km latitude/longitude/vertical grid, from pole-to-pole and 120–700 km. The results in C. Y. Lin, Lin, et al. (2020), J. T. Lin, Lin, et al. (2020) and Rajesh et al. (2021) demonstrate the quality of the GIS electron density in the 200–500 km altitude range and their ability to resolve day-to-day tidal variability in the ionosphere.

For the ionospheric tidal diagnostics, the GIS data, which are provided in geographic coordinates, are first mapped into altitude adjusted geomagnetic coordinates (Shepherd, 2014). The tidal spectrum is then computed by 2-D Fourier fitting the GIS electron density at each altitude and magnetic latitude using 1 day of data, producing amplitudes and phases every day. The single day spectrum is exemplified in Figure 1, for 6 January 2021, 20°N magnetic latitude and 380 km. Apart from the mean and the diurnal signal moving westward with the relative motion of the Sun, a rich spectrum of tidal signals is observed, including the semidiurnal migrating tide (zonal wavenumber = -2) and several nonmigrating tides.

To minimize artifacts from solar and geomagnetic activity, the amplitudes are then normalized with the zonal mean daily mean (wavenumber 0, frequency 0) part of the Fourier fit at each latitude and altitude, that is, relative amplitudes in percent are provided with respect to the mean at given magnetic latitude and altitude. Figures 2a and 2b shows the time evolution of the semidiurnal part of the tidal spectrum over the 145 day period from

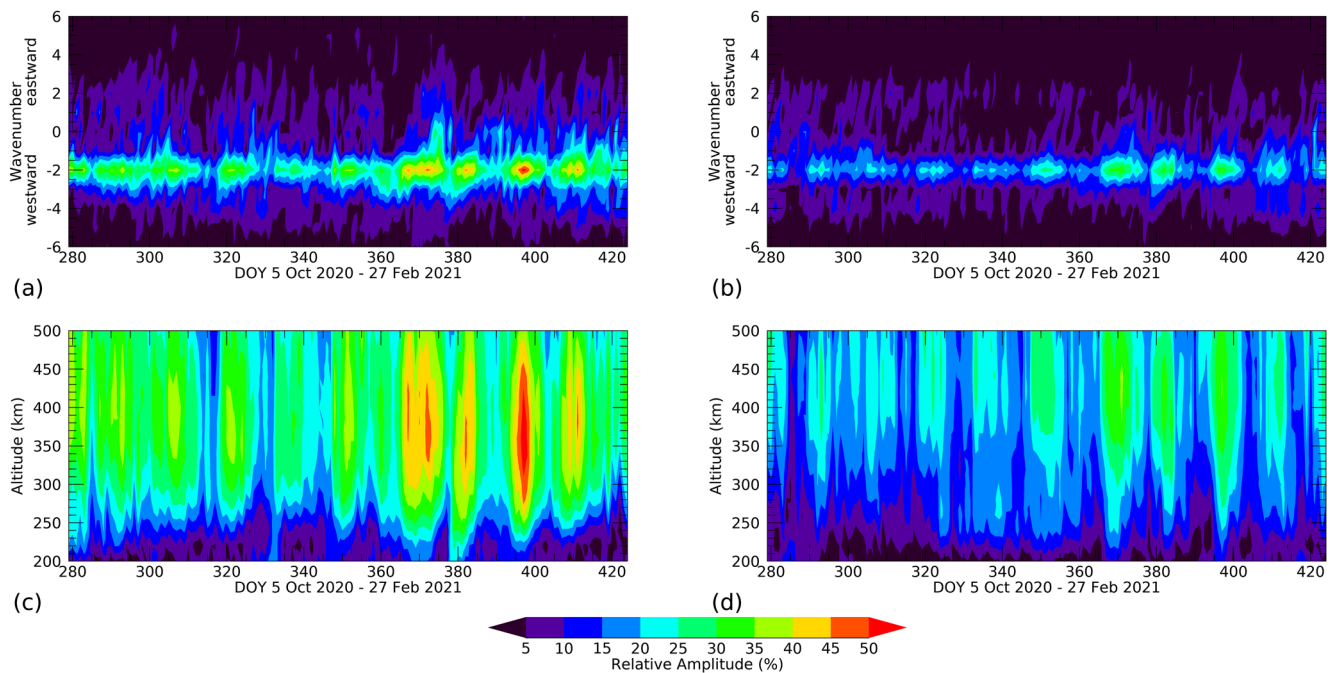


**Figure 2.** (a) Time evolution of the semidiurnal amplitude spectrum at 380 km and 20°N magnetic latitude. (b) Same as (a) but at 20°S magnetic latitude. (c) Semidiurnal migrating tide amplitude as function of time and altitude at 20°N magnetic latitude. (d) Same as (c) but for 20°S magnetic latitude. Plotted are relative amplitudes in percent, that is, relative to the zonal mean diurnal mean for each day, to remove geomagnetic variability effects.

day-of-year (DOY) 279 (5-October 2020) to DOY 424 (27-February 2021) at 20°N and 20°S magnetic latitudes (Equatorial Ionization Anomaly (EIA) crests) and 380 km, for zonal wavenumbers  $-6$  (westward propagation) to  $+6$  (eastward propagation). Note that the daily 2-D Fourier fitting of 1 hourly data does not allow one to separate between lunar (12.42 hr) and solar (12.0 hr) semidiurnal tides. The dominant semidiurnal migrating tide (zonal wavenumber  $-2$ ) is enhanced between DOY 365 to DOY 410 in both hemispheres but with substantial variations within a few days. A similar behavior is observed throughout the bottomside and topside (Figures 2c and 2d). In the following, the focus will be on the semidiurnal migrating tide, as this component is large and, from a modeling point of view, very sensitive to SSW in the E-region dynamo (N. Pedatella et al., 2014).

E-region dynamo tidal winds are analyzed from MIGHTI/ICON day and nighttime observations of zonal winds below 110 km altitude, data version v04, which have been validated against meteor radars (Harding et al., 2021). As a single satellite, ICON only covers two local solar times (LST) a day. ICON is in a 27° inclination orbit that precesses 29.8 min/day toward earlier LST. Cullens et al. (2020) show that 35 days of data have to be combined into a composite day to obtain a LST coverage sufficient for tidal diagnostics at all latitudes (10°S to 40°N) observed by MIGHTI. The tidal diagnostics of the composite data is further explained in (Forbes et al., 2022) and follows the same procedure as for TIDI tidal winds (Oberheide et al., 2006). It is important to note that the E-region tides from MIGHTI shown in the next Section 3 are running mean averages of 35-day of observation, in contrast to the “true” single day tides from COSMIC-2. Furthermore, the 35-day composite day approach for MIGHTI tides largely avoids “contamination” by the lunar semidiurnal tide: the latter is fully sampled in lunar local time over 9 consecutive days (Lieberman et al., 2022) such that the MIGHTI semidiurnal migrating tide is overwhelmingly from the solar part (SW2).

### 3. Discussion of SSW Response

The semidiurnal migrating tide or SW2 response to the SSW in the E-region zonal wind is shown in Figure 3, as a function of geographic latitude and DOY, for amplitudes (panel a) and phases (panel b). Overplotted as a black line is the 10 hPa zonal mean zonal wind at 60°N as a measure for the SSW. The polar stratospheric zonal winds reversed (SSW) between 5-January and 2-February with peak on 15-January and some intermittency on the order of 10 m/s within a few days. The low latitude SW2 enhancement during the SSW is quite evident even in the

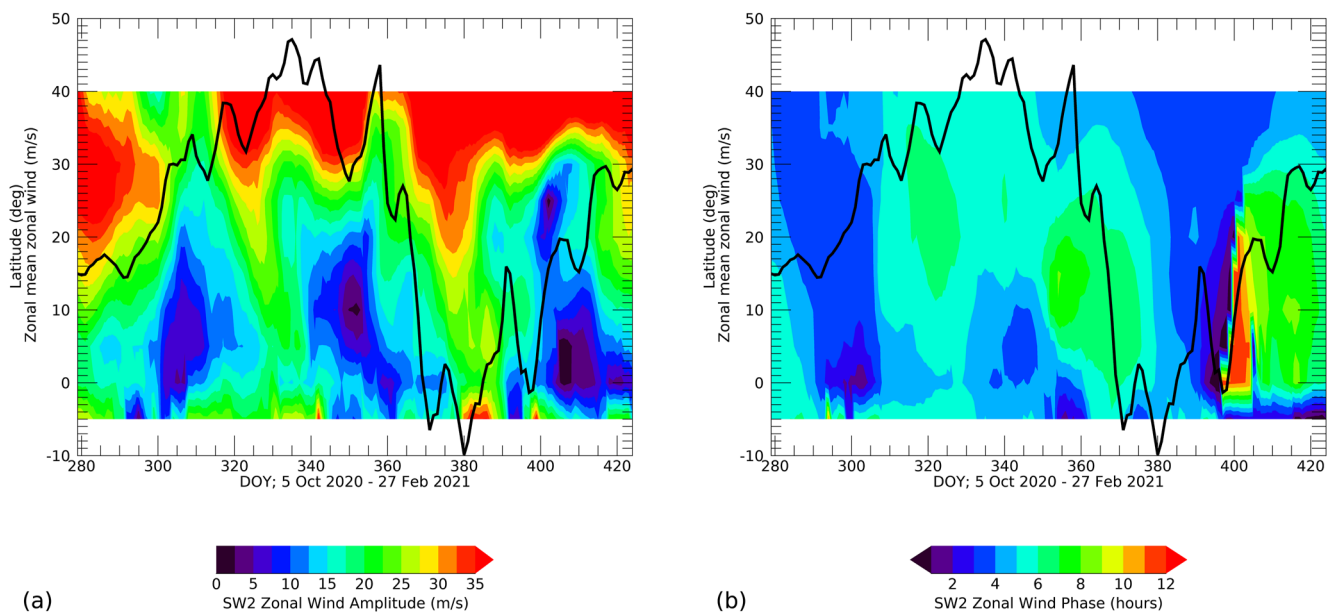


**Figure 3.** (a) Time evolution of the semidiurnal migrating tidal amplitudes in the zonal wind at 105 km from MIGHTI measurements. What is plotted are 35-day running means ( $\pm 17$  days around the day plotted) (b) Same as (a) but for tidal phases (universal time of maximum at  $0^\circ$  longitude). White areas indicate latitudes where tides cannot be derived from 35-day running mean composites. The black line in both panels is the zonal mean zonal wind at 10 hPa and  $60^\circ\text{N}$  from Modern-Era Retrospective analysis for Research and Applications, Version 2 (MERRA-2).

35-day running mean amplitudes, that is, from less than 10 m/s around DOY 340 to 30 m/s around DOY 375, at  $20^\circ\text{N}$  latitude. Tidal phases also shift by about 2–3 hr toward earlier times during the SSW. This is consistent with modeling expectations (N. Pedatella et al., 2014) of an SW2 phase shift during a SSW.

The corresponding F-region plasma response is shown in Figure 4, as a function of magnetic latitude and DOY. An important difference is that the GIS data allow one to resolve the “true” day-to-day variations in the tides, while Figure 3 is a 35-day running mean. Three relevant findings emerge from the comparison with the polar stratospheric zonal winds that are again overplotted as a thick line (now in white). Firstly, the overall semidiurnal amplitudes in the plasma are enhanced by about 2–3 color scales (about 10–15 percent points, or by more than 50% SSW to non-SSW). Secondly, the phases slightly shift toward earlier times during the SSW, consistent with the observed neutral wind phase behavior in the E-region. Thirdly, and this is perhaps the most unexpected finding, there is a very close match between even small variations in the polar stratospheric winds during the SSW and the F-region plasma response.

For example, the polar stratospheric wind change from  $-6.5$  m/s on 6-Jan (DOY 372) to  $+2.6$  m/s on 10-Jan (DOY 376) to  $-9.9$  m/s on 15-Jan (DOY 381). The corresponding northern EIA crest amplitudes change from 45% to 25% to 45%. Similarly, the polar stratospheric winds are  $+16$  m/s on 26-January (DOY 392),  $-1.3$  m/s on 1-February (DOY 398),  $+19.6$  m/s on 10-February (DOY 407),  $+15.2$  m/s on 14-February (DOY 411), with corresponding northern EIA amplitudes of about 20%, 50%, 20%, 45%, respectively. As such, even small inter-mittencies in the polar stratospheric winds during SSW, a.k.a., the rather complex position and elongation of the polar stratospheric vortex plays a critical role in the day-to-day variability of the F-region plasma. This finding is different to previous work (N. Pedatella, 2022) who used vertically integrated COSMIC-2 RO profiles during the 2021 SSW and interpreted short-term SW2 variations as beating between the solar and lunar semidiurnal migrating tides due to the length of the 5-day running mean analysis window. It is important to note that the day-to-day SW2 variability is not limited to the northern EIA crest but persists throughout all low and middle magnetic latitudes in both hemispheres and is similar in the bottomside F-region (compare Figure 2). The phases show a similar sensitivity: their day-to-day variability, while comparatively small, is nevertheless closely connected to the polar stratospheric vortex conditions. Solar and geomagnetic conditions do not play a role here as their day-to-day variability (Figure 4c) is very different to what is shown in Figures 4a and 4b.

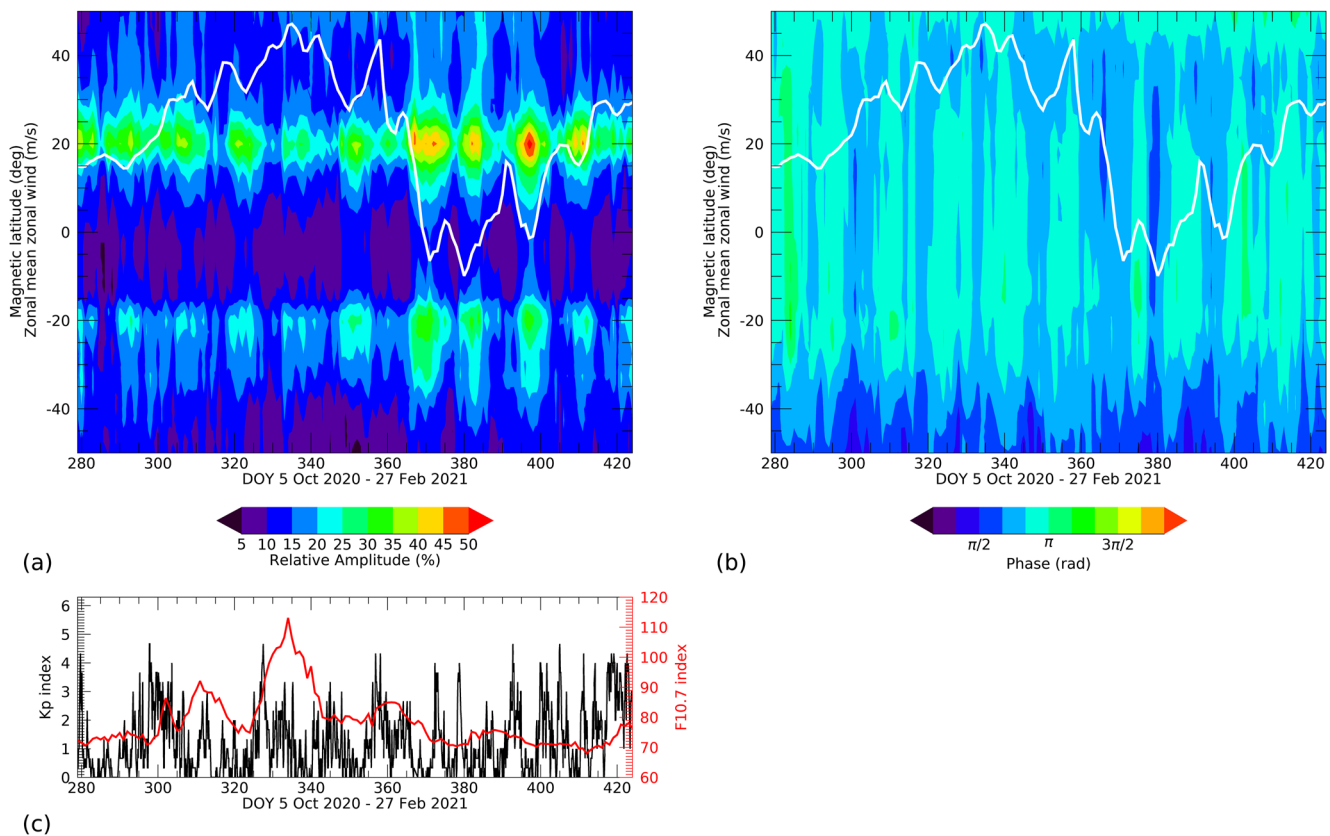


**Figure 4.** (a) Time evolution of the semidiurnal migrating tidal amplitudes from COSMIC-2 at 380 km as a function of magnetic latitude. (b) Same as (a) but for phases (rad of maximum). The white line in both panels is the zonal mean zonal wind at 10 hPa and 60°N from MERRA-2. Note the close correspondence of polar stratospheric winds and F-region electron density tides at all latitudes. (c) 3-hourly  $K_p$  index (black) and daily F10.7 index (red).

The most likely mechanism to transmit the SSW signal into the plasma is certainly through E-region dynamo modifications, as initially proposed by Goncharenko et al. (2010). E-region dynamo modulation is also the most likely explanation for the close correspondence between the day-to-day variations in the tidal wind and plasma amplitudes. N. M. Pedatella and Harvey (2022) recently reported a high correlation between the strength of the polar vortex and mesosphere/lower thermosphere tides from analyzing Microwave Limb Sounder (MLS) data and Specified Dynamics Whole Atmosphere Community Climate Model with thermosphere-ionosphere eXtension (SD-WACCMX) model simulations, with a semidiurnal tidal reduction of about 25% during strong polar vortex times. Their modeled daily SW2 variability during northern hemisphere winter showed a linear correlation of  $-0.62$  with daily variations in the strength of the polar vortex (expressed through the Northern Annular Mode). The COSMIC-2 observations in Figure 4 are consistent with this finding with linear correlations (DOY 360 to DOY 420) between the relative amplitudes and the plotted stratospheric wind of  $-0.47$ ,  $-0.60$ ,  $-0.64$  at 20°N, 0°N, 20°S magnetic latitude, respectively. Upward propagation meridional tidal winds and their day-to-day variability could play some role due to field-aligned plasma transport. But this question cannot be solved before day- and nighttime measurements can be made in the 110–200 km height region, to allow one to follow the height evolution of the semidiurnal tidal spectrum.

It is rather unlikely that thermospheric composition changes (as a source/sink of the plasma) play an important role in mapping the polar vortex strength variability into the F-region. The GOLD observations of the January 2019 SSW showed the importance of molecular diffusion for changing the mean state of upper thermospheric composition (Oberheide et al., 2020), but the changes were only on the order of 10% in 2019 (and 15% in 2021, not shown in this manuscript). Furthermore, diffusion causes a time delay of a few days between dynamical changes in the lower thermosphere (i.e., SSW-related changes in the wave-driving of the mean circulation) and the composition response in the upper thermosphere. There is no evidence for a time delay in Figure 4.

#### 4. Conclusions

The COSMIC-2 GIS data open a new window of opportunity to understand how weather-like variations from the lower atmosphere impact the global space weather of the ionosphere. The new capability to diagnose tides on a day-by-day basis shows a surprisingly close match with the strength of the polar vortex during a SSW, consistent with very recent modeling studies that connected mesosphere/lower thermosphere semidiurnal tidal variability with daily variations in the Northern Annual Mode. Polar vortex wind changes on the order of 5–10 m/s during the January 2021 SSW cause relative electron density semidiurnal tidal amplitudes to change by a factor of two within a few days. The comparison with 35-day running mean tidal diagnostics from ICON supports E-region dynamo modulation as the leading coupling mechanism while thermospheric composition can be ruled out through previous diagnostics of GOLD data. The broader implications of the present work is that the shown day-to-day variability in the COSMIC-2 tides is not limited to SSW events but can potentially be expanded to non-SSW periods and connected to the dynamics of the troposphere and stratosphere that can be predicted several days or weeks in advance (like the Northern Annual Mode).

#### Data Availability Statement

COSMIC-2 GIS data are publicly available after free registration at <http://formosat7.earth.ncku.edu.tw/>. Conversion into geomagnetic coordinates was performed using the 20191229 release of the AACGM-v2 software from Dartmouth University, available at <http://superdarn.thayer.dartmouth.edu/aacgm.html>. MIGHTI/ICON v04 winds were obtained from <https://icon.ssl.berkeley.edu/Data/Data-Product-Matrix> and GOLD O/N<sub>2</sub> data were obtained from <https://gold.cs.ucf.edu/data/search/>. The 3-hourly K<sub>p</sub> index was obtained from GFZ Potsdam at <https://www.gfz-potsdam.de/en/kp-index/> website, the F10.7 cm radio flux from NASA/GSFC OMNIWeb at <https://omniweb.gsfc.nasa.gov/form/dx1.html> website, and the MERRA-2 stratospheric zonal mean zonal winds at 60°N and 10 hPa from NASA/GSFC Atmospheric Chemistry and Dynamics Laboratory at [https://acd-ext.gsfc.nasa.gov/Data\\_services/met/ann\\_data.html](https://acd-ext.gsfc.nasa.gov/Data_services/met/ann_data.html) website.

#### References

- Cullens, C. Y., Immel, T. J., Triplett, C. C., Wu, Y.-J., England, S. L., Forbes, J. M., & Liu, G. (2020). Sensitivity study for ICON tidal analysis. *Progress in Earth and Planetary Science*, 7(18). <https://doi.org/10.1186/s40645-020-00330-6>
- Forbes, J. M., Oberheide, J., Zhang, X., Cullens, C., Englert, C. R., Harding, B. J., et al. (2022). Vertical coupling by solar semidiurnal tides in the thermosphere from ICON/MIGHTI measurements. *Journal of Geophysical Research: Space Physics*, 127(5), e2022JA030288. <https://doi.org/10.1029/2022JA030288>
- Forbes, J. M., & Zhang, X. (2012). Lunar tide amplification during the January 2009 stratosphere warming event: Observations and theory. *Journal of Geophysical Research*, 117(A12). <https://doi.org/10.1029/2012JA017963>
- Goncharenko, L. P., Chau, J. L., Liu, H.-L., & Coster, A. J. (2010). Unexpected connections between the stratosphere and ionosphere. *Geophysical Research Letters*, 37(10). <https://doi.org/10.1029/2010GL043125>
- Harding, B. J., Chau, J. L., He, M., Englert, C. R., Harlander, J. M., Marr, K. D., et al. (2021). Validation of ICON-MIGHTI thermospheric wind observations: 2. Green-line comparisons to specular meteor radars. *Journal of Geophysical Research: Space Physics*, 126(3), e2020JA028947. <https://doi.org/10.1029/2020JA028947>
- Jin, H., Miyoshi, Y., Pancheva, D., Mukhtarov, P., Fujiwara, H., & Shinagawa, H. (2012). Response of migrating tides to the stratospheric sudden warming in 2009 and their effects on the ionosphere studied by a whole atmosphere-ionosphere model GAIA with COSMIC and TIMED/SABER observations. *Journal of Geophysical Research*, 117(A10). <https://doi.org/10.1029/2012JA017650>
- Lieberman, R. S., Harding, B. J., Heelis, R. A., Pedatella, N. M., Forbes, J. M., & Oberheide, J. (2022). Atmospheric lunar tide in the low latitude thermosphere-ionosphere. *Geophysical Research Letters*, 49(11), e2022GL098078. <https://doi.org/10.1029/2022GL098078>
- Lieberman, R. S., Riggins, D. M., Orland, D. A., Oberheide, J., & Siskind, D. E. (2015). Global observations and modeling of nonmigrating diurnal tides generated by tide-planetary wave interactions. *Journal of Geophysical Research: Atmospheres*, 120(22), 11419–11437. <https://doi.org/10.1002/2015JD023739>
- Lin, C.-Y., Lin, C. C.-H., Liu, J.-Y., Rajesh, P. K., Matsuo, T., Chou, M.-Y., et al. (2020). The early results and validation of FORMOSAT-7/COSMIC-2 space weather products: Global ionospheric specification and Ne-aided Abel electron density profile. *Journal of Geophysical Research: Space Physics*, 125(10), e2020JA028028. <https://doi.org/10.1029/2020JA028028>
- Lin, C. Y., Matsuo, T., Liu, J. Y., Lin, C. H., Huba, J. D., Tsai, H. F., & Chen, C. Y. (2017). Data assimilation of ground-based GPS and radio occultation total electron content for global ionospheric specification. *Journal of Geophysical Research: Space Physics*, 122(10), 10876–10886. <https://doi.org/10.1002/2017JA024185>
- Lin, J. T., Lin, C. H., Lin, C. Y., Pedatella, N. M., Rajesh, P. K., Matsuo, T., & Liu, J. Y. (2019). Revisiting the modulations of ionospheric solar and lunar migrating tides during the 2009 stratospheric sudden warming by using global ionosphere specification. *Space Weather*, 17(5), 767–777. <https://doi.org/10.1029/2019SW002184>
- Lin, J. T., Lin, C. H., Rajesh, P. K., Yue, J., Lin, C. Y., & Matsuo, T. (2020). Local-time and vertical characteristics of Quasi-6-day oscillation in the ionosphere during the 2019 Antarctic sudden stratospheric warming. *Geophysical Research Letters*, 47(21), e2020GL090345. <https://doi.org/10.1029/2020GL090345>

#### Acknowledgments

This work was supported by NASA grants 80NSSC22K1010, 80NSSC22K0018 and NSF Award 2149695.

- Liu, G., Janches, D., Ma, J., Lieberman, R. S., Stober, G., Moffat-Griffin, T., et al. (2022). Mesosphere and lower thermosphere winds and tidal variations during the 2019 Antarctic sudden stratospheric warming. *Journal of Geophysical Research: Space Physics*, *127*(3), e2021JA030177. <https://doi.org/10.1029/2021JA030177>
- Oberheide, J., Forbes, J. M., Zhang, X., & Bruinsma, S. L. (2011). Climatology of upward propagating diurnal and semidiurnal tides in the thermosphere. *Journal of Geophysical Research*, *116*(A11). <https://doi.org/10.1029/2011JA016784>
- Oberheide, J., Pedatella, N. M., Gan, Q., Kumari, K., Burns, A. G., & Eastes, R. W. (2020). Thermospheric composition O/N<sub>2</sub> response to an altered meridional mean circulation during Sudden Stratospheric Warmings observed by GOLD. *Geophysical Research Letters*, *47*(1), e2019GL086313. <https://doi.org/10.1029/2019GL086313>
- Oberheide, J., Wu, Q., Killeen, T. L., Hagan, M. E., & Roble, R. G. (2006). Diurnal nonmigrating tides from TIMED Doppler Interferometer wind data: Monthly climatologies and seasonal variations. *Journal of Geophysical Research*, *111*(A10), A10S03. <https://doi.org/10.1029/2005JA011491>
- Pediatella, N. (2022). Ionospheric variability during the 2020–2021 SSW: COSMIC-2 observations and WACCM-X simulations. *Atmosphere*, *13*(3), 368. <https://doi.org/10.3390/atmos13030368>
- Pediatella, N., Liu, H.-L., Sassi, F., Lei, J., Chau, J., & Zhang, X. (2014). Ionosphere variability during the 2009 SSW: Influence of the lunar semidiurnal tide and mechanisms producing electron density variability. *Journal of Geophysical Research: Space Physics*, *119*(5), 3828–3843. <https://doi.org/10.1002/2014JA019849>
- Pediatella, N. M., & Forbes, J. M. (2010). Evidence for stratosphere sudden warming-ionosphere coupling due to vertically propagating tides. *Geophysical Research Letters*, *37*(11). <https://doi.org/10.1029/2010GL043560>
- Pediatella, N. M., & Harvey, V. L. (2022). Impact of strong and weak stratospheric polar vortices on the mesosphere and lower thermosphere. *Geophysical Research Letters*, *49*(10), e2022GL098877. <https://doi.org/10.1029/2022GL098877>
- Rajesh, P. K., Lin, C. C. H., Lin, J.-T., Lin, C.-Y., Yue, J., Matsuo, T., et al. (2021). Day-to-day variability of ionospheric electron density during solar minimum derived from FORMOSAT-7/COSMIC-2 measurements. *Terrestrial, Atmospheric and Oceanic Sciences*, *32*(6.1), 1–17. <https://doi.org/10.3319/TAO.2021.08.01.01>
- Sathishkumar, S., & Sridharan, S. (2013). Lunar and solar tidal variabilities in mesospheric winds and EEJ strength over Tirunelveli (8.7°N, 77.8°E) during the 2009 major stratospheric warming. *Journal of Geophysical Research: Space Physics*, *118*(1), 533–541. <https://doi.org/10.1029/2012JA018236>
- Shepherd, S. G. (2014). Altitude-adjusted corrected geomagnetic coordinates: Definition and functional approximations. *Journal of Geophysical Research: Space Physics*, *119*(9), 7501–7521. <https://doi.org/10.1002/2014JA020264>
- Yamazaki, Y., Matthias, V., Miyoshi, Y., Stolle, C., Siddiqui, T., Kervalishvili, G., et al. (2020). September 2019 Antarctic sudden stratospheric warming: Quasi-6-Day wave burst and ionospheric effects. *Geophysical Research Letters*, *47*(1), e2019GL086577. <https://doi.org/10.1029/2019GL086577>
- Yamazaki, Y., & Richmond, A. D. (2013). A theory of ionospheric response to upward-propagating tides: Electrodynamic effects and tidal mixing effects. *Journal of Geophysical Research: Space Physics*, *118*(9), 5891–5905. <https://doi.org/10.1002/jgra.50487>